Int. J. Electrochem. Sci., 9 **(2014)** 6352 - 6358

International Journal of
ELECTROCHEMICAL
SCIENCE
www.electrochemsci.org

Short Communication

Photoinduced Nonlinear Optical Second –Order Optical Effects in the Ag-ZnO Nanorods

A. H.Reshak[1,2,3,*], *Sin Tee Tan*[4], *Fitri Yeni Naumar*,[4] *A.A.Umar*[4], *M.Oyama*[5], *Z. A. Alahmed*[6], *H. Kamarudin*[2], *I.V.Kityk*[7]

[1]New Technologies - Research Center, University of West Bohemia, Univerzitni 8, 306 14 Pilsen, Czech Republic
[2] Center of Excellence Geopolymer and Green Technology, School of Material Engineering, University Malaysia Perlis, 01007 Kangar, Perlis, Malaysia
[3] Institute of Complex systems, FFPW, CENAKVA-South Bohemia University CB, Nove Hrady 37333, Czech Republic
[4]Institute of Microengineering and Nanoelectronics, Universiti Kebangsaan Malaysia, 43600 UKM Bangi, Selangor, Malaysia
[5]Department of Material Chemistry, Graduate School of Engineering, Kyoto University, Nishikyo-ku, Kyoto 615-8520, Japan
[6] Department of Physics and Astronomy, King Saud University, Riyadh 11451, Saudi Arabia
[7] Department of Physics, Eastern Ukrainian National University, 13 Voli Ave., Lutsk 43025, Ukraine
[*]E-mail: maalidph@yahoo.co.uk

Received: 19 November 2013 / *Accepted:* 3 August 2014 / *Published:* 25 August 2014

ZnO nanorods with controlled-surface density have been successfully obtained by simply varying the concentration of the growth solution. It was found that the variation in the growth solution concentration may vary the surface density of the ZnO nanorods arrays grown on the surface. The lowest concentration produces the lowest nanorods surface density. The photoinduced second harmonic generation was studied for the nanosecond Er:glass lasers at wavelength 1540 nm and induced by bicolour treatment at 1540/770 nm wavelengths. The nonlinear dependence on the Ag NP presence was observed. And it s was substantially higher than for the pure ZnO nanoparticles.

Keywords: synthesis of ZnO nanorods; silver nanoprticles. Optical properties.

1. INTRODUCTION

The ZnO nanoparticles cause recently enhanced interst as promisng materials for nonlinear otpics [1]. This is caused by a very specific features of their interfaces which give additional contribution to the corresponding hyperpolarizablities. Particular interest presents second-order optical susceptibilities like second harmonic generation [2] described by third-order tensor components. It

was established that the correspond effects were very sensitive to the sizes and the topology of nanorods [3]. Particular interest present the ZnO nanoparticles with attached noble metallic nanoparticles [4]. Due to presence of surface plasmon resonances one can expect a possibility of occurrence of enhanced second-order optical effects which may be additionally stimulated by external laser light. As a consequence in the present work we will perform studies of the photoinduced second harmonic generation in the ZnO nanorods doped with the different content of silver nanoparticles.

2. METHODOLOGY

2.1 Preparation of Ag nanoparticles-loaded ZnO nanorods (Ag-ZnO nanorods)

Ag nanoparticles-loaded ZnO nanorods array were grown on a FTO substrate surface via a two-step processes. Namely growth of ZnO nanorods array on FTO surface and attachment of Ag nanoparticle onto the ZnO nanorods surface. ZnO nanorods array were prepared using a two steps wet-chemical processes, namely seeding and growth processes [5-7]. Seeding process is the process of attachment of ZnO nanoseed (size approximately 5-10 nm) on the substrate surface that was achieved using an alcholthermal approach, our previously reported method [8-10]. In typical procedure, an ethanoloic solution of zinc nitrate hexahydrate (Sigma Aldrich) with concentration of 0.01 M was firstly prepared. After that, 90 μL of the solution was spin-coated onto the FTO substrate at 3000 rpm for 30 sec. The sample was then baked on a hot plate at 100 ˚C for 15 min to facilitate a proper attachment of zinc salt precursor on the surface. These procedures were repeated 3 times to obtain a homogeneous layer of chemical precursor on the FTO surface. The sample was then transferred into an electrical oven for annealing process in air at 350 ˚C for 1 hour. Using these procedures, high-density ZnO nanoseed with size dimensions approximately equal to 5 to 10 nm can be realized on the surface. The ZnO nanorods were then projected from the attached nanoseed via a microwave-assisted hydrolysis method, using a 5 mL aqueous growth solution that consists of equimolar (0.04 M) of zinc nitrate hexadehydrate and hexamethylenetetramine (HMT, Sigma Aldrich). In typical growth process, the nanoseed –attached FTO substrate was transferred into a Teflon sealed glass vial containing the growth solution. The reaction was then put into a Panasonic inverted home application microwave oven and irradiated with 1100 W of microwave for 20 seconds. The sample was then taken out, rinsed with copious amount of pure water and finally dried with a flow of nitrogen gas. Using this approach, white fluffy colour was noticed on the FTO surface, indicating the formation of ZnO nanorods array on the surface. The ZnO nanorods array sample with a different surface density was obtained by simply preparing the sample in a growth solution with different concentrations, namely from 0.01 to 0.05 M.

Finally, the Ag nanoparticles was attached onto the surface of the ZnO nanorods array using our previously reported method [11] by simply immersing the sample into a 20 mL aqueous solution of equimolar (0.25 mM) of silver nitrate (Sigma Aldrich) and Trisodium citrate (Wako Pure Chemicals, Ltd.). The process was left undisturbed for 30 min. After that, 0.5 mL of 0.1 M ice-cooled $NaBH_4$ (Wako Pure Chemicals, Ltd.) was added into the solution. At this stage, the colour of the solution change from transparent to yellow, inferring the formation of Ag nanoparticles both in the solution and on the surface of ZnO nanorods array. These systems were then kept undisturbed for an hour at room temperature (ca. ~25 °C). The sample was then taken out, rinsed with copious amount of pure water

and finally dried with a flow of nitrogen gas. A yellowish colour was noticed on the substrate surface, indicating the successful attachment of Ag nanoparticles on the ZnO nanorods surface. Finally, the sample was then annealed in air at 200 ^{0} C for 1 h to remove any organic residues on the surface.

2.2 Characterisations

The morphology of Ag nanoparticle-loaded ZnO nanorods arrays was examined using field emission electron microscope (FESEM, Hitachi S-4800) that operates at accelerating voltage of 2 kV. The optical absorption properties of the sample was obtained from UV-Vis- NIR Spectrometer (Perkin Elmer, Lambda 900).

3. RESULTS AND DISCUSSION

3.1 Ag-ZnO nanorods preparation and characterization

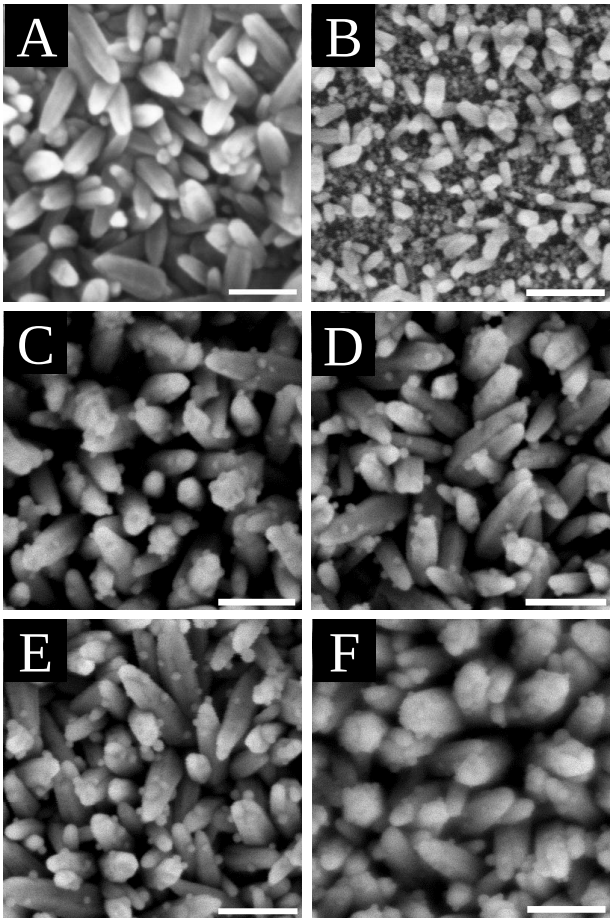

Figure 1. (A) is typical FESEM image of ZnO nanorods without Ag nanoparticles loading that prepared using the growth solution with concentration of 0.03 M. FESEM images of Ag-ZnO nanorods with different ZnO nanorods surface density that are prepared using the growth solution containing equimolar of zinc nitrate hexahydrate and hexamethylenetetramine of 0.01 M (B), 0.02 M (C), 0.03 M (D), 0.04 M (E) and 0.05 M (F). Red circle in the B to F are showing typical Ag nanoparticle attached on the ZnO nanorods. Scale bars are 100 nm.

Figure 1 shows typical FESEM images of Ag nanoparticles-loaded ZnO nanorods with several nanorods surface density obtained using the present method. As seen from the Figure 1 A-E, Ag nanoparticle with size approximately 5 ± 1.0 nm have been effectively attached onto the surface of the ZnO nanorods (see red circle in corresponding image). The FESEM image of ZnO nanorods without Ag nanoparticles loading is shown in Figure 1F for comparison. Following the Figure 1 at least 5 Ag nanoparticle attached onto the surface of the nanorods. Based on our previous study, the attachment characteristic of organic-capped metallic nanostructures, such as used in the present work, only involve weak van der Waals interaction instead of strong chemical bonding with the substrate surface. This condition may produce novel and unique optical and electrical properties and has shown a prospective performance in non-linear optical [12], sensing [13] and catalysis applications [14].

As also judged from the image in Figure 1, a controlled-surface density of ZnO nanorods have been successfully obtained by simply varying the concentration of the growth solution. It was found that the variation in the growth solution concentration may vary the surface density of the ZnO nanorods arrays growth on the surface. For example, the lowest concentration (see Figure 1A) produces the lowest in the nanorods surface density. Surface analysis using image of software on this result has shown that the surface density of the nanorods is as high as approximately 200 nanorod/ μm^2.

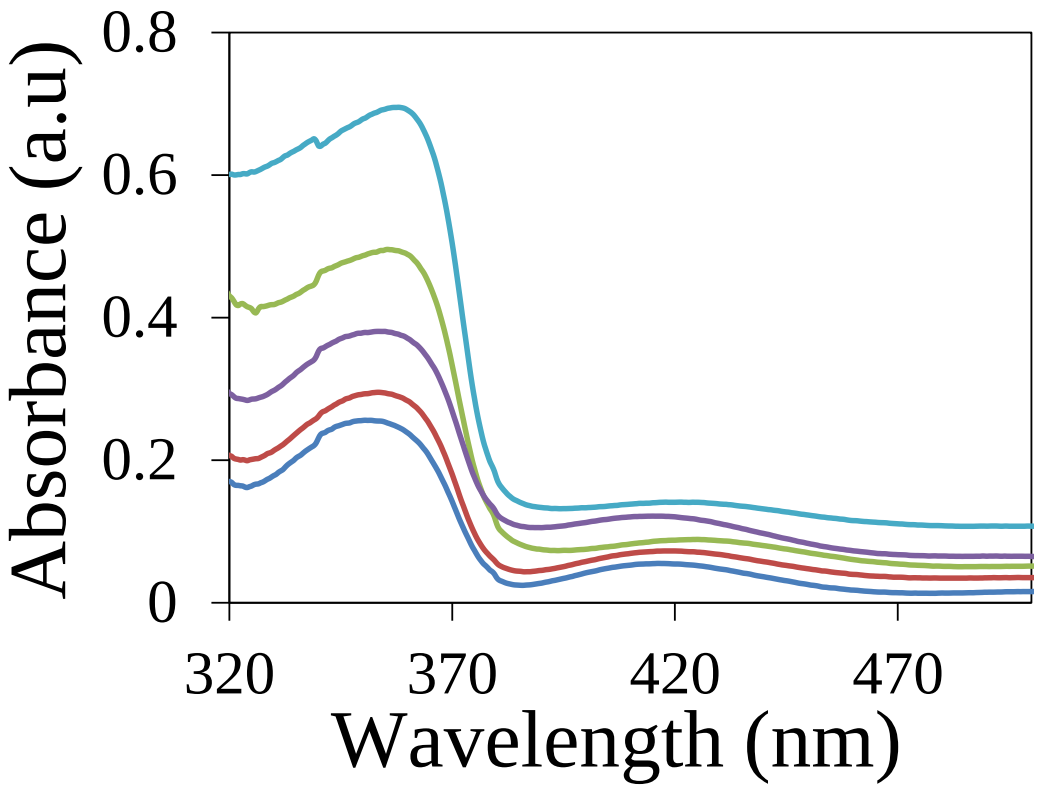

Figure 2. UV-VIS spectra of Ag nanoparticle-loaded ZnO nanorods grow on the FTO substrate with different nanorods surface density.

The density effectively increased to 250, 290, 300 and 320 nanorods per μm^2 when the concentration was increased from 0.01 M to 0.02, 0.03, 0.04 and 0.05 M, respectively. Similar to the variation on the surface density, the change in the growth solution concentration also modified the diameter of the nanorods array. In typical process, the lowest concentration was found to produce nanorods with diameter of approximately 11.0 ± 1.0 nm. The nanorods diameter increased with the increasing of growth solution concentration, namely to 21.0 ± 1.5, 25.0 ± 0.4, 34.0 ± 1.7 and 38.00 ± 1.0 nm when the concentration increased to 0.02, 0.03, 0.04 and 0.05 M, respectively. The nanorods diameter adopted the Gaussian distribution function.

The variation in the surface density and the diameter of the nanorods upon growth solution concentration change can be associated with the effect of competitive growth process of the nanoseed under a highly kinetic nature of the growth process [15-17]. As has been mentioned earlier, in the growth process, relatively similar nanoseed surface density on the substrate surface was used to project the nanorods growth. Under a kinetic growth process and a highly competitive nature, every nanoseed may have similar opportunity but competitive to project the nanorods growth. Therefore, the diameter as well as the nanorods surface density increases with the increasing of the growth solution concentration. However, at relatively low concentration, such competitive nature of the growth process is quite intense. This condition only facilitates a quicker growth of the growing site instead of every nanoseed on the surface. Thus, scarce nanorods formation on the surface was obtained.

While FESEM image show the unique Ag-ZnO nanorods structural growth with different surface density on the substrate surface, the UV-Vis optical absorption spectra exhibits a peculiar optical absorption properties of the structure, the result of effective Ag nanoparticle loading on the ZnO nanorods array. The results are shown in Figure 2. As the Figure 2 shows, the entire sample exhibits the presence of two absorption bands in the spectrum csituated at 361 and 419 nm. The higher energy band can be easily associated with the excitonic optical absorption band of ZnO. Meanwhile, the lower absorption band is the surface Plasmon resonance absorption band of Ag nanoparticles. As also can be seen from the Figure 2, the absorbance of the samples, independent of the wavelength, increase with the increasing of nanorods surface density. However, interestingly, the absorption peak position is un-shifted with the increasing of the nanorods surface density. This is a clear evidence of the effective improvement of the nanorods surface density instead of increasing the nanorods aggregation on the surface [18]. Thus, no shift in the absorption peak position of the sample observed when the nanorods surface density increased. Similar phenomenon is also observed in the surface Plasmon band of the Ag nanoparticles. The increase in the nanorod surface density also produce the increase in the surface density of Ag nanoparticles loading. However, the Ag nanoparticles aggregation is also predicted to be limited. This condition might produce peculiar performance in linear and non-linear optical applications.

The photoinduced SHG was performed in the reflected regime . As a source laser 15 ns Er-glass laser was used. The optimal ratio between the fundamental and the doubled frequency beams was equal to 6:1. The phototreatement by the bicolor laser beams was performed using from 2 up to 4 min. up to the achievement of the maximal SHG. The latter was detected by red interference filter at 770 nm. The detection was performed by photomultiplier with Hamamatsu photomultiplier and using the

Tectronix oscilloscope. The reference signal was obtained for the ZnO NP with sizes about 30 nm and is present ion the Fig. 3.

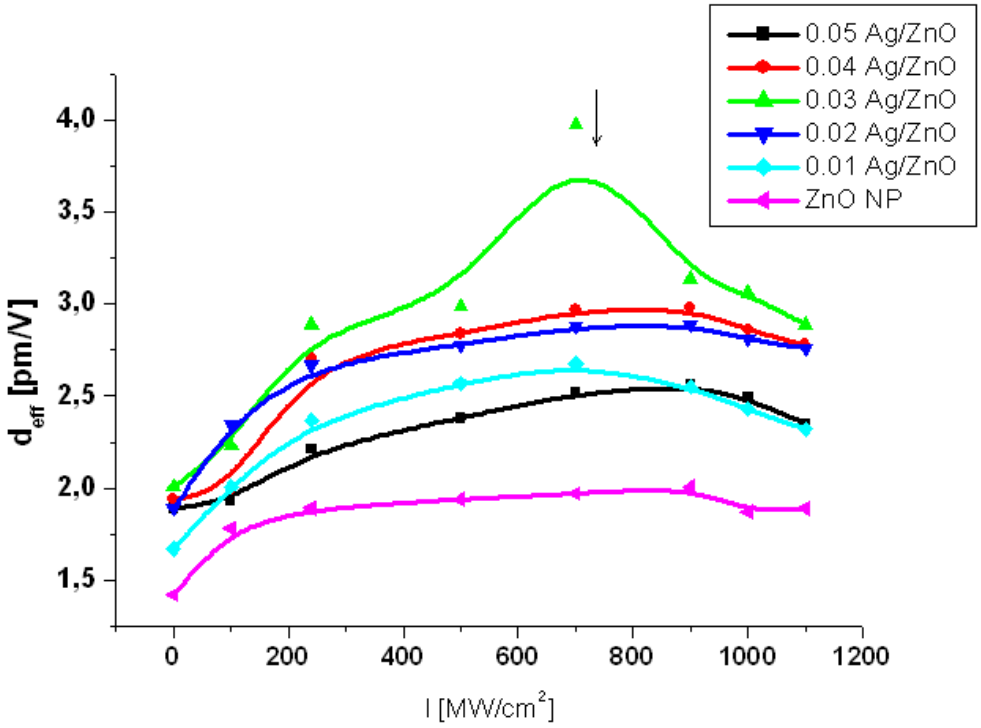

Figure 3. Photoinduced dependence of the second-order susceptibilities for the Ag/ZnO NP versus the bicolor treatment by 1540 nm/770 nm nanosecond Er-glass laser pulses.

The presented data unambiguously show that there exists substantial influence of the Ag on the output SHG. The maximal signal was obtained for the nanocomposites 0.02 Ag/ZnO. The maximal SHG output was achieved at power densities about 720 MW/cm^2. The further decrease may be caused by photo thermal destroying of the photoinduced gratings which also is related to the large number of nano-trapping levels.

4. CONCLUSIONS

It was found that the variation in the growth solution concentration may vary the surface density of the ZnO nanorods arrays growth on the surface. The lowest concentration produces the lowest in the nanorods surface density. The photoinduced SHG was performed in the reflected regime . As a source laser 15 ns Er-glass laser was used. The optimal ratio between the fundamental and the doubled frequency beams was equal to 6:1. The phototreatement by the bicolor laser beams was performed using from 2 up to 4 min. up to the achievement of the maximal SHG. The latter was detected by red interference filter at 770 nm. there exists substantial influence of the Ag on the output SHG. The maximal signal was obtained for the nanocomposites 0.02 Ag/ZnO. The maximal SHG

output was achieved at power densities about 720 MW/cm^2. The further decrease may be caused by photo thermal destroying of the photoinduced gratings which also is related to the large number of nano-trapping levels.

ACKNOWLEDGEMENTS
The result was developed within the CENTEM project, reg. no. CZ.1.05/2.1.00/03.0088, co-funded by the ERDF as part of the Ministry of Education, Youth and Sports OP RDI program. Computational resources were provided by MetaCentrum (LM2010005) and CERIT-SC (CZ.1.05/3.2.00/08.0144) infrastructures.

References

1. S-K Min, C-H Oh, G. J. Lee, Y. P. Lee, *Journal of the Korean Physical Society*, 55 (2009) 1005-1008
2. Xiao Si, Su Xiong-Rui, Li Chun, Han Yi-Bo, Fang Guo-Jia and Wang Qu-Quan., *Chinese Physics* B. 17 (2008) 1291
3. G. Wang, G. T. Kiehne, G. K. L. Wong and J. B. Ketterson, *Appl. Phys. Lett*. 80 (2002) 401; X. Q. Zhang, Z. K. Tang, M. Kawasaki, A. Ohtomo, H. Koinuma, *J. Phys.: Condens. Mater*. 15 (2003) 5191-5196; U. Neumann, R. Grunwald, U. Griebner and G. Steinmeyer, *Appl. Phys. Lett*. 84 (2004)170.
4. K. Ozga, T. Kawaharamura, A. Ali Umar, M. Oyama, K. Nouneh, A. Slezak, S. Fujita, M. Piasecki, A. H. Reshak, I.V.Kityk, *Nanotechnology*, 19 (2008) 185709
5. A. A. Umar, M. Oyama, *Appl Surf Sci*, 253 (2006) 2196-2202
6. A.A. Umar, M. Oyama, *Crystal Growth and Design*, 7 (2007) 2404-2409.
7. A.A. Umar, M. Oyama, *Crystal Growth and Design*, 5 (2005) 599-607.
8. S.T. Tan, A.A. Umar, M. Yahaya, M.M. Salleh, C.C. Yap, H.-Q. Nguyen, C.-F. Dee, E.Y. Chang, M. Oyama, *Sci Adv Mater*, 5 (2013) 803-809.
9. S. Tan, A. Umar, M. Yahaya, C. Yap, M. Salleh, *Journal of Physics: Conference Series*, (2013) 12001-12008.
10. A.A. Umar, M.Y.A. Rahman, R. Taslim, M.M. Salleh, M. Oyama, *Nanoscale Res Lett*, 6 (2011) 1-12.
11. J. Ebothe, K. Ozga, A. Ali Umar, M. Oyama, I.V. Kityk, *Appl Surf Sci*, 253 (2006) 1626-1630.
12. K. Ozga, M. Oyama, M. Szota, M. Nabialek, I.V. Kityk, A. Slzak, A.A. Umar, K. Nouneh, *J Alloy Compd*, 509 (2011) S424-S426.
13. A.A. Ibrahim, G.N. Dar, S.A. Zaidi, A. Umar, M. Abaker, H. Bouzid, S. Baskoutas, *Talanta*, 93 (2012) 257-263.
14. W. Xie, Y. Li, W. Sun, J. Huang, H. Xie, X. Zhao, *Journal of Photochemistry and Photobiology A: Chemistry*, 216 (2010) 149-155.
15. L. Vayssieres, *Adv Mater*, 15 (2003) 464-466.
16. L. Vayssieres, K. Keis, A. Hagfeldt, S.E. Lindquist, *Chem Mater*, 13 (2001) 4395
17. Y. Yang, Y. Yang, H. Wu, S. Guo, *Crystengcomm*, 15 (2013) 2608-2615.
18. A. Demortiere, P. Launois, N. Goubet, P.A. Albouy, C. Petit, *J Phys Chem* B, 112 (2008) 14583-14592.